The Journal of Physiology

Exercise and hypoxia unmask pulmonary vascular disease and right ventricular dysfunction in a 10- to 12-week-old swine model of neonatal oxidative injury

Jarno J. Steenhorst[1,2], Alexander Hirsch[1,2], Annemarie Verzijl[1], Piotr Wielopolski[2], Daphne de Wijs-Meijler[1], Dirk J. Duncker[1], Irwin K. M. Reiss[3] and Daphne Merkus[1,4,5]

[1]*Division of Experimental Cardiology, Department of Cardiology, Erasmus MC, University Medical Center Rotterdam, Rotterdam, the Netherlands*
[2]*Department of Radiology and Nuclear Medicine, Erasmus MC, University Medical Center Rotterdam, Rotterdam, the Netherlands*
[3]*Division of Neonatology, Department of Pediatrics, Erasmus MC, University Medical Center Rotterdam, Rotterdam, the Netherlands*
[4]*Institute for Surgical Research, Walter Brendel Center of Experimental Medicine (WBex), University Clinic Munich, LMU Munich, Munich, Germany*
[5]*German Center for Cardiovascular Research, Partner Site Munich, Munich Heart Alliance, Munich, Germany*

Handling Editors: Laura Bennet & Janna Morrison

The peer review history is available in the Supporting information section of this article (https://doi.org/10.1113/JP282906#support-information-section).

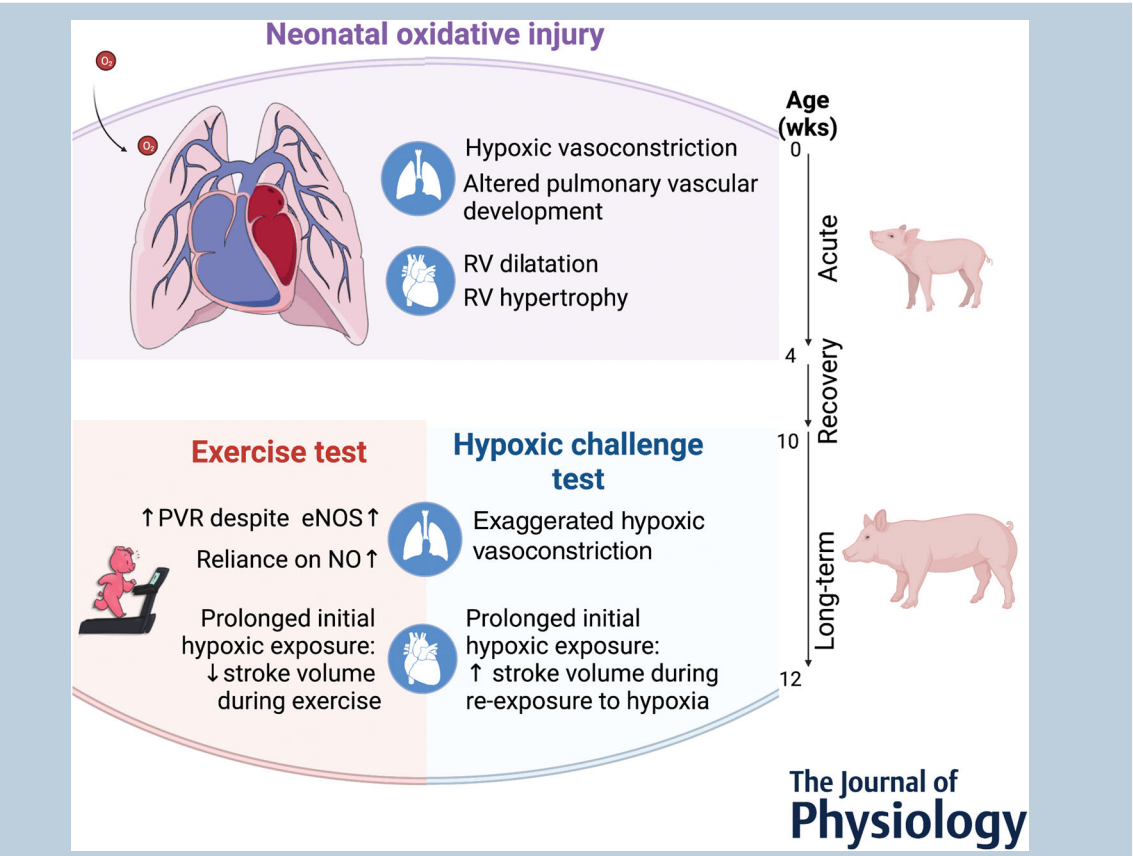

Abstract Prematurely born young adults who experienced neonatal oxidative injury (NOI) of the lungs have increased incidence of cardiovascular disease. Here, we investigated the long-term effects of NOI on cardiopulmonary function in piglets at the age of 10–12 weeks. To induce NOI, term-born piglets (1.81 ± 0.06 kg) were exposed to hypoxia (10–12% F_{iO_2}), within 2 days after birth, and maintained for 4 weeks or until symptoms of heart failure developed (range 16–28 days), while SHAM piglets were normoxia raised. Following recovery (>5 weeks), NOI piglets were surgically

DOI: 10.1113/JP282906

instrumented to measure haemodynamics during hypoxic challenge testing (HCT) and exercise with modulation of the nitric-oxide system. During exercise, NOI piglets showed a normal increase in cardiac index, but an exaggerated increase in pulmonary artery pressure and a blunted increase in left atrial pressure – suggesting left atrial under-filling – consistent with an elevated pulmonary vascular resistance (PVR), which correlated with the duration of hypoxia exposure. Moreover, hypoxia duration correlated inversely with stroke volume (SV) during exercise. Nitric oxide synthase inhibition and HCT resulted in an exaggerated increase in PVR, while the PVR reduction by phosphodiesterase-5 inhibition was enhanced in NOI compared to SHAM piglets. Finally, within the NOI piglet group, prolonged duration of hypoxia was associated with a better maintenance of SV during HCT, likely due to the increase in RV mass. In conclusion, duration of neonatal hypoxia appears an important determinant of alterations in cardiopulmonary function that persist further into life. These changes encompass both pulmonary vascular and cardiac responses to hypoxia and exercise.

(Received 27 January 2022; accepted after revision 18 July 2022; first published online 21 July 2022)
Corresponding author D. Merkus: Division of Experimental Cardiology, Department of Cardiology, Erasmus MC, University Medical Centre Rotterdam, PO Box 2040, 3000 CA, Rotterdam, the Netherlands. Email: d.merkus@erasmusmc.nl

Abstract figure legend Exposure of neonatal swine to hypoxia for up to 4 weeks resulted in an increase in pulmonary vascular resistance (PVR) and right ventricular (RV) hypertrophy that persisted after recovery in normoxia. Exercise experiments revealed an increased dependency on nitric oxide (NO) to maintain a low PVR, as well as a reduced stroke volume during exercise. Re-exposure to hypoxia showed an exaggerated increase in PVR, but stroke volume was better maintained in neonatal hypoxia-exposed animals. eNOS, endothelial nitric oxide synthase.

Key points

- Children who suffered from neonatal oxidative injury, such as very preterm born infants, have increased risk of cardiopulmonary disease later in life.
- Risk stratification requires knowledge of the mechanistic underpinning and the time course of progression into cardiopulmonary disease.
- Exercise and hypoxic challenge testing showed that 10- to 12-week-old swine that previously experienced neonatal oxidative injury had increased pulmonary vascular resistance and nitric oxide dependency.
- Duration of neonatal oxidative injury was a determinant of structural and functional cardiopulmonary remodelling later in life.
- Remodelling of the right ventricle, as a result of prolonged neonatal oxidative injury, resulted in worse performance during exercise, but enabled better performance during the hypoxic challenge test.
- Increased nitric oxide dependency together with age- or comorbidity-related endothelial dysfunction may contribute to predisposition to pulmonary hypertension later in life.

Jarno J. Steenhorst is an MD-trained PhD candidate in the departments of Pediatric and Experimental Cardiology in the Erasmus MC. In collaboration with multiple departments, he is involved in clinical and pre-clinical studies to understand the influence of neonatal injury of the lungs on long term cardiopulmonary functional and structural outcomes. The current work investigates cardiopulmonary consequences of neonatal oxidative injury, predisposing swine to structural and functional alterations that might be of relevance during late hits to the cardiopulmonary system.

Introduction

Preterm birth is associated with an increased risk in cardiopulmonary disease later in life (Crump et al., 2019; Greer et al., 2021; Zoller et al., 2015). A growing body of evidence shows that prematurely born infants – with and without neonatal chronic lung disease – exhibit a distinct cardiovascular risk profile in childhood and adulthood (Duke et al., 2021; Lewandowski, Bradlow et al., 2013; McKay et al., 2021; Telles et al., 2020). Several studies found a higher incidence of pulmonary arterial hypertension (PAH) and ischaemic heart disease compared to term born, healthy adults (Crump et al., 2019; Naumburg & Soderstrom, 2019; Zoller et al., 2015). Knowing if, how and when prematurely born young adults could progress into PAH or heart disease is critical to be able to intervene at early stages.

Young adult survivors of prematurity exhibit higher pulmonary arterial pressure (PAP), accompanied by a blunted exercise response, which is associated with cardiac remodelling (Corrado, Barton, Macdonald et al., 2021; Crispi et al., 2021; Goss et al., 2018). However, conflicting results have been published concerning the structural and functional cardiac phenotype in these patients. Some studies report higher right ventricular (RV) mass and hyper-contractility, while others report lower RV mass and a decrease in contractile function, fuelling an ongoing debate in the literature on cardiac phenotype of ex-prematurity (Bates et al., 2020; Goss & Eldridge, 2021; Goss et al., 2020; Lewandowski & Levy, 2021; Lewandowski, Augustine et al., 2013). Duration of perinatal oxidative injury seems to be a key contributor to the pulmonary vascular and cardiac remodelling observed in humans and animal models (Goss et al., 2015, 2018).

Immediately following birth, the pulmonary circulation experiences a dramatic increase in flow when lungs are aerated. In the subsequent period, the pulmonary vasculature undergoes vascular growth and remodelling, resulting in a further decrease in pulmonary vascular resistance (PVR). Oxidative injury during the early postnatal period impairs this growth and remodelling, resulting in a higher PVR. In a swine model, previously developed by our group, we observed that 4 weeks of hypoxia (10–12% fraction of inspired oxygen (F_{iO_2})) shortly after birth, resulted in pulmonary hypertension that persisted for several weeks after return to normoxia (de Wijs-Meijler et al., 2018). PAP eventually decreased to normal levels after return to normoxia, suggesting transient neonatal pulmonary vascular disease (PVD). Male piglets were more susceptible to develop persistent PVD. Remarkably, a large heterogeneity in tolerance for the duration of the hypoxia period was observed, with high mortality rates in the third and fourth week of hypoxic exposure, attributed to RV failure (de Wijs-Meijler et al., 2018).

Based on these observations, we hypothesized that insults on the pulmonary vasculature in this transition period shortly after birth, impairing the postnatal decrease in resistance, while still requiring the accommodation of a large increase in pulmonary blood flow, contribute importantly to risk for development of cardiopulmonary disease later in life. Consequently, in the present study, we investigated in 10- to 12-week-old chronically instrumented swine whether neonatal PVD has a lasting impact on the cardiopulmonary system, with persistent structural and functional cardiopulmonary abnormalities. Secondly, we assessed the influence of duration of early post-natal hypoxic exposure on the development of distinct structural and functional cardiac phenotypes. To unmask cardiopulmonary abnormalities, we utilized (1) re-exposure to hypoxia and (2) graded treadmill exercise with a focus on alterations in the nitric oxide pathway.

Methods

Experiments were performed in accordance with the *Guiding Principles in the Care and Use of Laboratory Animals* as approved by the Council of the American Physiological Society and with approval of the Animal Care Committee of Erasmus MC, University Medical Center Rotterdam (AVD101002016636).

Twenty-four male Yorkshire × Landrace piglets, born at term at a commercial breeder (Roefs, Woensdrecht, The Netherlands), were taken from the sow at 36−48 h after birth. After arrival in our institute, all piglets received a single dose of artificial colostrum (Colo-active Plus, Schippers BV, Bladel, The Netherlands) and pig pusher (MS Pig Pusher Oral, Schippers BV, Bladel, The Netherlands) on day 2, 3 and 5. The experimental protocol was adapted from our previous study (de Wijs-Meijler et al., 2018), and is shown in Fig. 1.

Induction of neonatal oxidative injury

Upon arrival in the facility, piglets were placed in an incubator (2 m^2), in which the fraction of inspired oxygen could be regulated using a N_2 generator (AV5-TT606SC, Avilo, Dirksland, The Netherlands). Upon arrival in the facility, 14 piglets (1.81 ± 0.08 kg) were assigned to the neonatal oxidative injury (NOI) group and were exposed to normobaric hypoxia with an F_{iO_2} of 10% in the first week, followed by a weekly increase in F_{iO_2} of 0.5% per week to a maximum of 12%. Ten piglets weighing 1.80 ± 0.05 kg, $P = 0.2105$) were assigned to the control group (SHAM) and were placed in the same incubator but under normobaric, normoxic conditions. Piglets were fed every hour using an automated feeding system with age-appropriate artificial milk (Lactowean Extra

and Babywean, Denkavit, Voorthuizen, The Netherlands). After 1 week, solid food for small piglets was introduced (Mellow Go and Top Wean, Denkavit).

At week 2, 3, 4 and 8, piglets underwent echocardiography (Zonare ZS3, Mindray Medical, Hoevelaken, The Netherlands) under sedation (mixture of 3−5% sevoflurane and 95−97% oxygen) during spontaneous breathing. Cardiac function and progression of pulmonary hypertension were assessed using para- and substernal views. The protocol included tricuspid regurgitation peak velocity (TR_{vel}), tricuspid annular plane systolic excursion (TAPSE), pulmonary artery acceleration time (PAAT) and left ventricular (LV) eccentricity index (defined as anterior–posterior diameter divided by free wall-septal wall diameter). TAPSE values were normalized to RV length. Echocardiograms were assessed for intermediate or high pulmonary hypertension probability. Intermediate probability was defined as TR_{max} >2.0 m s^{-1} and/or eccentricity index >1. High probability was defined as TR_{max} >3.5 m s^{-1} and/or eccentricity index >1.4.

Piglets were checked for clinical symptoms of cardiac dysfunction twice per day. Moderate dysfunction was defined as a flattening in growth curve, lethargy and dyspnoea on exertion. Severe dysfunction was defined as feeding withdrawal, stable weight >2 days, weight loss >1 day and dyspnoea at rest.

To reduce mortality, NOI piglets were placed in a normoxic environment if they exhibited clinical symptoms and echocardiographic signs of pulmonary hypertension after at least 14 days of hypoxia. When intermediate probability of pulmonary hypertension was observed during echocardiography, piglets were returned to normoxia when severe clinical symptoms occurred. When high probability was observed during echocardiography, moderate clinical symptoms were sufficient to return to normoxia. After 4 weeks of hypoxia exposure, piglets were returned to normoxia, even if end-points as described above were not met. In the normoxic environment, the number of feeds was gradually reduced to two servings per day. Water was available *ad libitum*.

At least 2 weeks after return to normoxia, NOI and SHAM piglets were familiarized with exercising on the treadmill for 3−5 min, ∼3 times per week, to prevent distress during the subsequent exercise experiments.

Cardiovascular magnetic resonance imaging

Piglets underwent cardiovascular magnetic resonance (CMR) at two time points during the protocol (Fig. 1). At least 2 days, but maximally 1 week after return to normoxia (depending on availability of MRI), the NOI group underwent CMR, whereas SHAM piglets underwent CMR at 4–5 weeks of age. With heart-failure symptoms typically developing in less than 4 weeks, this may have resulted in a small age-dependent bias, for which we corrected by indexing for weight of the piglets. Twelve out of 14 NOI piglets and six out of 10 SHAM piglets underwent CMR at week 12 just before sacrifice.

Piglets were sedated with an intramuscular cocktail of xylazine (1.75 mg kg^{-1}), tiletamine-zolazepam (3 mg kg^{-1}) and atropine (0.50 mg). Piglets were intubated and intravenous access was obtained via an ear vein. Thiopental (50 mg ml^{-1}) was slowly injected to achieve breathing suppression. Piglets were transported to the CMR, while being ventilated with a mobile ventilator (Carina, Dräger Medical, Best, The Netherlands), placed in right lateral position and ventilated through extended

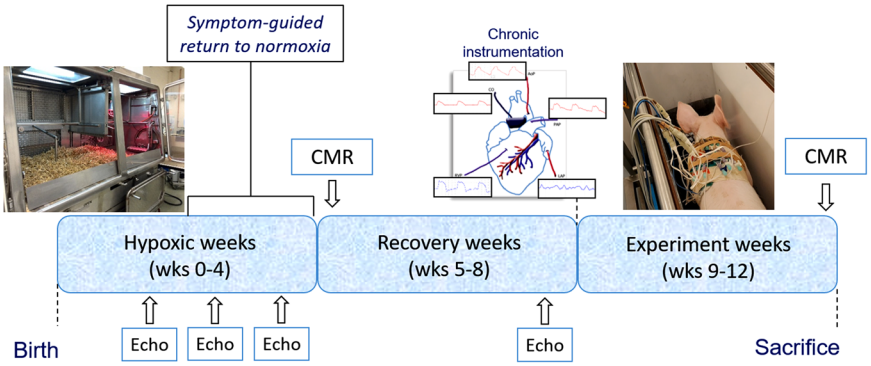

Figure 1. Schematic overview of the protocol
Neonatal oxidative injury (NOI) is induced by placing piglets in hypoxia (10–12% fraction of inspired oxygen) for a maximum of 28 days. After initial recovery (<7 days), swine underwent cardiovascular magnetic resonance (CMR) under anaesthesia. At the start of week 9, piglets were chronically instrumented. The exercise and hypoxic challenge experiments (photograph insets) took place from week 10 onward until the second CMR and sacrifice after week 12. SHAM operated piglets followed the same protocol, but were not subjected to hypoxia in the first 28 days. [Colour figure can be viewed at wileyonlinelibrary.com]

tubing connecting the endotracheal tube to the ventilator placed outside the CMR suite. A coupling piece with a valve ensured that expiration occurred directly into the ambient space at the site of the endotracheal tube, thereby avoiding dead space ventilation. Breath-holds could manually be applied from the operating room. Due to the lack of arterial access (first CMR) and long distance between the CMR suite and the laboratory (second CMR), no blood samples were taken for blood gas analysis during CMR. CMR was performed on a 1.5 T clinical scanner with a dedicated 32-channel phased-array surface coil (SIGNA artist, GE Healthcare, Milwaukee, WI, USA). The imaging protocol consisted of retrospectively ECG-gated 2D balanced Steady-State Free Precession cine imaging with breath-hold. Standard long-axis and short-axis images with full LV and RV coverage were obtained. Typical scan parameters were slice thickness 6.0 mm, slice gap 0 mm, field of view 240−320 × 168−224, repetition time/echo time 3.8/1.5 ms, flip angle 60°, NEX 1, acquired matrix 280 × 200 mm, and number of reconstructed phases 30 per cardiac cycle to maintain temporal resolution <45 ms. The planning of the short axis cine images was done according to a standardized imaging protocol used in every scan, parallel to the mitral valve planned at both the four- and two-chamber views and perpendicular to the long axis of the body of the left ventricle. Short axis slices were acquired from base to apex with several slices above the mitral valve to have complete coverage of both the left and right ventricle and outflow tracts (see Fig. 2). To assess mass and volumes, endo- and epicardial contours were manually drawn on end-diastolic and end-systolic short axis cine images. Volumes were measured and ejection fraction was calculated. All volumes and mass were indexed for body weight. RV global longitudinal strain (GLS) was measured using the four-chamber longitudinal axis by manually drawing endo- and epicardial contours during end-diastole and end-systole of the RV with subsequent automatic tracking during the entire cardiac cycle. The analyses were done with QMass (version 8.1) and Qstrain (version 2.0) analytical software from Medis Medical Imaging Systems BV (Leiden, The Netherlands).

Surgical procedure

At 9 weeks of age, animals were sedated and intubated as described above and were ventilated with extra F_{IO_2} (30–45%) and sevoflurane (2–3%) to induce adequate anaesthesia. To achieve proper analgesia, sufentanil (10 μg kg^{-1} h^{-1} I.V.) was administered. Depth of anaesthesia was checked regularly using a pain stimulus, while heart

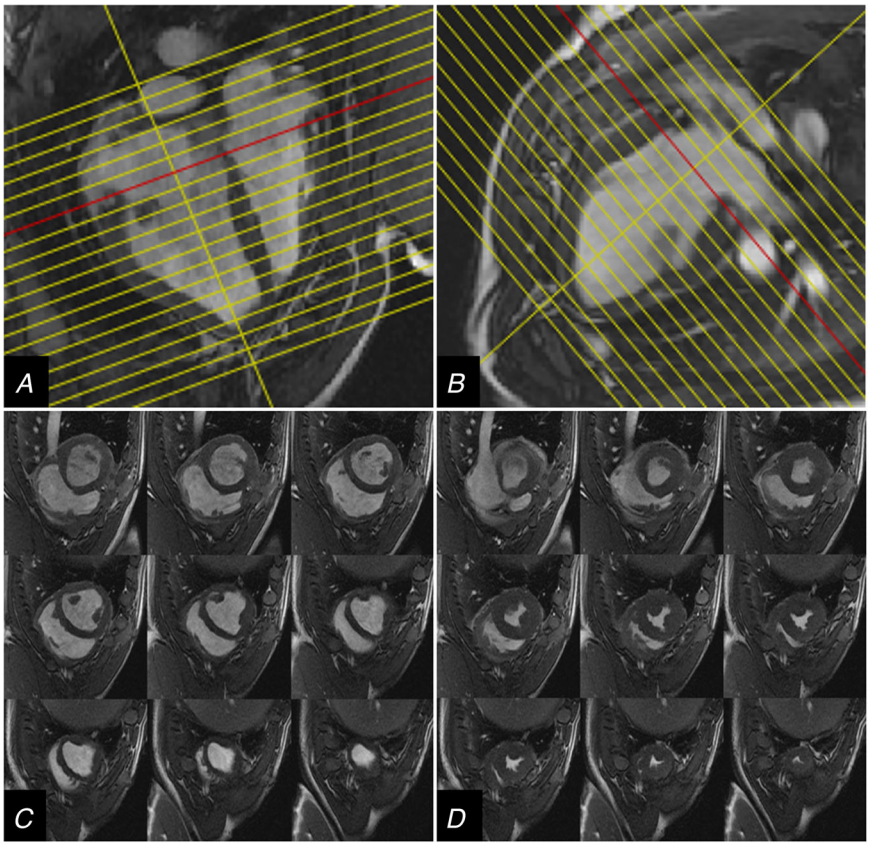

Figure 2. Planning of the MRI
A and *B*, planning of the short axis plane parallel to the mitral valve in the 4-(*A*) and 2-chamber (*B*) long axis plane and perpendicular to the long-axis of the left ventricle. *C* and *D* nine short axis cine slices of the ventricles in end-diastole (*C*) and end-systole (*D*). [Colour figure can be viewed at wileyonlinelibrary.com]

rate and end-tidal CO_2 were monitored continuously. Piglets were instrumented under sterile conditions as previously described in detail (De Wijs-Meijler et al., 2016). Briefly, the chest was opened through the fourth left intercostal space, and fluid-filled polyvinylchloride catheters were inserted through puncture holes into the descending aorta, left atrium, pulmonary artery, RV and LV and secured in place using a purse string suture. Catheters were used for pressure measurements, blood sampling and drug infusion. A transit time flow-probe (16 mm, Transonic Systems, Ithaca, NY, USA) was placed around the ascending aorta for measurement of cardiac output. Catheters and flow probe wire were tunnelled subcutaneously to the back, and the chest was closed in layers. All animals received buprenorphine (0.015 mg kg^{-1} I.M.) once and a fentanyl 72 h slow-release patch (6 μg h^{-1}) for analgesia, as well as Augmentin (25/5 mg kg^{-1} I.V.) for 7 days as antibiotic prophylaxis. All catheters were flushed daily with heparinized saline (1000–5000 IU ml^{-1} saline) to maintain patency (De Wijs-Meijler et al., 2016). Following chronic instrumentation, pigs were individually housed with free access to water. Visual and nose–nose contact was possible through Plexiglas with holes between pens.

In vivo haemodynamic measurements

For haemodynamic measurements, fluid-filled pressure transducers (Combitrans, B Braun Medical BV, OSs, The Netherlands) were attached to the catheters, placed on the back of the piglet and calibrated at mid-chest level. Resting haemodynamic measurements were continuously recorded using a CODAS workstation (ATCODAS, Dataq Instruments, Akron, OH, USA) and heart rate, cardiac output, aortic pressure, PAP, left atrial pressure (LAP), RV pressure and LV pressure) were obtained using MATLAB (The MathWorks Inc., Natick, MA, USA) (De Wijs-Meijler et al, 2016).

Hypoxic challenge test

Upon completion of baseline haemodynamic measurements, an arterial blood sample was taken in room air. The piglet was then placed in a box (300 l, pre-filled with hypoxic gas mixture) for re-exposure to hypoxia. The pressure catheters and flow probe wire were tunnelled through a small opening in the box and connected to the pressure transducers for continuous pressure and cardiac output measurements. F_{iO_2} in the box was continuously monitored, while a mixture of N_2 and O_2 was added to the box with high flow (15 l min^{-1}) until 14−15% F_{iO_2} was reached and the experiment started. Haemodynamic measurements and arterial blood samples were taken at 2, 5, 10, 15 and 20 min. The box was opened after the measurement at 20 min, followed by two recovery measurements and blood samples at 25 and 30 min after the initial start of the hypoxic challenge test (HCT).

Exercise experiments

Haemodynamic measurements were recorded at rest in a standing position, and arterial and venous blood samples and rectal temperature were obtained. Piglets were subsequently subjected to a four-stage exercise protocol (1–4 km h^{-1} for 3 min per speed). Haemodynamic variables were continuously recorded, while blood samples were obtained in the last 60 s of each 3-min exercise level, when cardiopulmonary steady state had been achieved. Blood gas analysis consisting of (rectal) temperature corrected oxygen and carbon dioxide tension, haemoglobin concentration and oxygen saturation was performed using an ABL-800 (Radiometer, Copenhagen, Denmark).

After at least 1 h of rest, piglets repeated the exercise protocol in the presence of nitric oxide synthase (NOS) inhibition (20 mg kg^{-1} of N^{ω}–nitro-L-arginine (L-NNA, Sigma-Aldrich, St Louis, MO, USA) intravenously) or phosphodiesterase 5 (PDE5) inhibition (0.16 mg kg^{-1} sildenafil (Revatio, Pfizer Inc, New York, NY, USA) I.V.). Exercise runs with a pharmacological intervention were compared to the closest control exercise experiment (performed preferably on the same day) without a pharmacological intervention.

Termination

Piglets were sedated with premedication (xylazine (1.75 mg kg^{-1}), tiletamine-zolazepam (3 mg kg^{-1}) and atropine (0.50 mg)) through I.M. injection. Piglets were intubated and thiopental was slowly infused until breathing suppression was achieved. To maintain anaesthesia, piglets were artificially ventilated with sevoflurane 2−3% and received sufentanil (10 μg kg^{-1} h^{-1}) intravenously. A sternotomy was performed and ventricular fibrillation was induced by using a 9 V battery. The heart and lungs were excised, ventricles were weighed and tissues were prepared and stored for further analysis.

Histology

Samples were excised from the RV wall and fixed in 4% buffered formaldehyde and embedded in paraffin for histological analyses. RV wall sections (4.0 μm thick) were stained for quantification of myocardial collagen deposition, myocyte size and capillary density as previously published (van de Wouw et al., 2021). Six to

Table 1. Genes with primers used for qPCR

Gene	Forward sequence	Reverse sequence
ACTB	TCCCTGGAGAAGAGCTACGA	AGCACCGTGTTGGCGTAG
CYPA	AGACAGCAGAAAACTTCCGTG	AAGATGCCAGGACCCGTATG
COL1a1	AGACATCCCACCAGTCACCT	TCACGTCATCGCACAACACA
COL3a1	AATCATGCCCTACTGGTGGC	CGGGTCCAACTTCACCCTTA
MMP-2	GCAGTGATGGCAAGTTGTGG	TTGACATCGTCGTGGGACAG

Abbreviations: *ACTB*, actin beta; *COL1a1*, collagen type 1; *COL3a1*, collagen type 3; *CYPA*, cyclophilin A; *MMP-2*, metalloprotease 2.

eight fields were examined in the endocardial part of each slide, at ×20 magnification. Interstitial collagen deposition was assessed using picrosirius red staining, with perivascular collagen deposition being excluded from the analysis. The areas occupied by collagen fibre were measured and expressed as a percentage of the myocardial area. Cross-sectional areas of cardiomyocytes with clearly visible nuclei were measured for each slide, using a Gomori silver stain. All measurements were performed using a microscopy image analysis system (Impak C, Clemex Vision Image analysis system, Clemex Technologies, Quebec, Canada) and by a blinded observer.

The accessory lobe of the lungs was inflated and perfusion fixated through the trachea with 4% buffered formaldehyde with a pressure of 25 cmH_2O. Sections (4.0 μm thick) were excised and vascular structure was assessed using a Resorcin–Fuchsin–Van Gieson's staining. Whole section images were obtained using the Hamamatsu NanoZoomer Digital Pathology (NDP) slide scanner (Hamamatsu Nanozoomer 2.0HT, Hamamatsu Photonics K.K., Hamamatsu City, Japan). A blinded observer measured internal and external elastic lamina areas of small pulmonary arteries (20–60 μm in diameter) using NPD viewer (Hamamatsu). Assuming circularity of the vessels, inner and outer radius were calculated as: $r = \sqrt{(\text{area}/\pi)}$. Wall-to-lumen ratio was calculated as (outer − inner radius)/inner radius.

Molecular analysis

Expression of genes involved in collagen synthesis and degradation was determined in snap frozen RV tissue. Total RNA was analysed from and RV tissue. The Minimum Information for Publication of Quantitative Real-Time PCR Experiments (MIQE) guidelines were followed (Bustin et al, 2009). Specifically, RNA purity and concentration were measured and cDNA (SensiFAST cDNA synthesis kit, Bioline, London, UK) synthesis was used to with 500 ng RNA as input. Only RNA with RNA integrity number >8.5 was used. The CFX96 Real-Time PCR detection system (Bio-Rad Laboratories, Hercules, CA, USA) was used to analyse gene expression, using the SensiMix SBR-green supermix (Bioline). Table 1 shows the primers used. All genes were normalized using cyclophilin A and β-actin as housekeeping genes as these were more stable than *GAPDH* and *RPL13A*. All primers were tested for linear amplification (efficiency 90−110%) and PCR products were sequenced at least once to confirm amplification of the correct target genes.

Western blot

In snap frozen bulk lung tissue from the middle lobe of the right lung, total endothelial NOS (eNOS) and phosphorylated eNOS (Ser1177 site) were determined by SDS-PAGE. Proteins were transferred to nitrocellulose membranes and blots were probed with primary anti-phospho-eNOS Ser1177 (1:1000, purified monoclonal rabbit anti-human eNOS, CST9570, Cell Signaling Technology Inc., Danvers, MA, USA), anti-eNOS (1:500, purified monoclonal mouse anti-human eNOS, 610297, Transduction Laboratory, BD Biosciences, San Jose, CA, USA), and anti-glyceraldehyde 3-phosphate dehydrogenase (GAPDH; 1:1000, 14C10, Cell Signaling Technology). All blots were analysed using the Odyssey CLX imaging system (LI-COR Biotechnology, Lincoln, NE, USA). We performed Rout's test on the data, which identified one outlier in the NOI group.

Haemodynamic measurements

Off-line analysis of haemodynamics was performed using CODAS and a program written in MATLAB. Haemodynamic data were averaged over 10 s. Cardiac index was calculated as cardiac output/weight. PVR was defined as (PAP − LAP)/cardiac index. Stroke volume was calculated as cardiac index/heart rate. RV dP/dt_{max} was defined as the maximum rate of rise of RV pressure, while RV dP/dt_{min} was defined as maximum rate of fall of RV pressure. Body oxygen consumption ($B\dot{V}_{O_2}$) was computed as cardiac index × (arterial O_2 content − mixed venous O_2 content). Data from the control runs (i.e. runs without pharmacological interventions) were averaged for comparison between groups. Measurements during HCT (at 2, 5, 10, 15 and 20 min) were averaged and compared to baseline values.

Statistics

All statistical analyses were performed in SPSS Statistics version 25 (IBM Corp., Armonk, NY, USA) and Prism version 8 (GraphPad Software Inc., San Diego, CA, USA). Continuous parametric variables (according to a Shapiro–Wilk test) are presented as means ± standard deviation (SD), while differences between baseline values of the two groups were tested by a Student's *t* test. Continuous non-parametric variables are presented as median (interquartile range) and tested by a Kruskal–Wallace test. A mixed-model ANOVA was used to analyse the longitudinal HCT and exercise data. Linear univariate regression modelling was performed on cardiopulmonary outcomes using duration of hypoxic exposure within the NOI group as predictor. A value of $P < 0.05$ (two-tailed) was considered to be statistically significant.

Results

Duration of hypoxic exposure and survival

One piglet was taken out of the hypoxic chamber at day 10 with severe diarrhoea and excluded from further analysis. Of the 13 remaining NOI piglets, 12 met the end-points for early return to normoxia during the hypoxic period. Despite return to normoxia, heart failure did not resolve in one piglet at 2 weeks of hypoxic exposure, while three more piglets had to be euthanized because of severe heart failure (one at 6 weeks and two more at 11 weeks into the protocol, just prior to the final CMR). One NOI piglet died shortly after the first CMR from a non-cardiac-related cause. In the SHAM group, three piglets died during surgery.

RV imaging and structure

Echocardiography showed that F_{iO_2} of 10−12% resulted in an increase in TR_{vel} and LV eccentricity index, while TAPSE decreased, consistent with the presence of pulmonary hypertension (Table 2). During CMR shortly after return to normoxia, stroke volume was maintained in NOI piglets compared to SHAM piglets, but NOI piglets showed impaired RV function (decrease in GLS) and compensatory RV hypertrophy (increase in RV mass). At 8 weeks of age, that is at least 4 weeks after return to normoxia, TR_{vel}, LV eccentricity index and TAPSE normalized. At 12 weeks of age, that is at least 2 months after return to normoxia, CMR showed recovery of RV GLS as well (Table 2). Nevertheless, post-mortem weighed RV mass was still higher in NOI piglets compared to SHAM piglets (1.8 ± 0.1 *vs.* 1.5 ± 0.1 g kg^{-1}, $P = 0.004$) and correlated with the duration of hypoxic exposure (Fig. 3). Global RV hypertrophy was accompanied by increased cardiomyocyte cross-sectional area in NOI piglets (9.2 ± 0.5 *vs.* 7.3 ± 0.5 μm^2 kg^{-1}, $P = 0.011$), which did not correlate with duration of hypoxic exposure.

Total collagen area, as well as mRNA levels of COL1a1 and COL3a1, MMP2 and MMP9 in the RV were not different between NOI and SHAM piglets (Fig. 3). However, there was a negative correlation between RV mRNA of the COL3a1, coding for the more compliant collagen type 3, as well as for MMP2 with duration of hypoxic exposure.

Resting haemodynamics

At 10−12 weeks of age, no significant differences were found in heart rate, cardiac index, PAP and LAP between groups under resting conditions (Table 3). Resting PVR was significantly higher in NOI piglets compared to SHAM and correlated with duration of hypoxic exposure (Fig. 4). However, histological analyses showed no increased muscularization of the pulmonary vasculature, as wall-to-lumen ratios were similar in both groups (SHAM 0.17 ± 0.05 *vs.* NOI 0.16 ± 0.05, $P = 0.953$, Fig. 4).

Hypoxic challenge test

During acute re-exposure to hypoxia, NOI piglets showed a lower LAP and a larger increase in PAP and PVR compared to SHAM piglets, which was predominantly seen in the first 5 min of re-exposure to hypoxia (Table 3, Fig. 5). The exaggerated increase in PVR in NOI piglets during the HCT did not appear to be influenced by the duration of postnatal hypoxic exposure. Re-exposure to hypoxia decreased stroke volume to the same extent in both groups. Interestingly, prolonged postnatal hypoxic exposure (>20 days) actually prevented the decrease in stroke volume despite the marked increase in afterload (Fig. 5), possibly aided by the higher RV mass in NOI piglets with the longest exposure to hypoxia (Fig. 3).

Haemodynamics during exercise

Similar to resting conditions, no significant differences between SHAM and NOI piglets were observed in mean levels of heart rate, CI and stroke volume during exercise (Table 3). Interestingly, during heavy exercise we observed an inverse correlation between stroke volume and the duration of hypoxia in the NOI group (Fig. 5), which is likely due to the higher PAP during exercise in NOI compared to SHAM piglets. The higher PAP, together with a lower LAP (Table 3) while CI was maintained, implies a higher PVR in NOI for any given level of $B\dot{V}_{O_2}$ (Fig. 5). Notably, PVR difference between NOI and SHAM trended to increase during exercise, suggesting a lack of pulmonary vascular recruitment in NOI compared to SHAM piglets.

Table 2. Cardiac imaging throughout the protocol

	SHAM	*n*	Neonatal oxidative injury	*n*	*P*
Week 2					
Weight (kg)	3.4 ± 0.3	8	2.9 ± 0.2	13	**0.0001**
TAPSE	0.35 ± 0.07	8	0.24 ± 0.06	12	**0.0008**
TR_{vel} (m s^{-1})	1.5 ± 0.7	7	2.9 ± 1.0	12	**0.0024**
LV ED eccentricity index	1.0 ± 0.1	7	1.4 ± 0.2	12	**<0.0001**
LV ES eccentricity index	1.0 ± 0.1	8	1.5 ± 0.4	12	**0.0038**
Week 4					
Weight (kg)	7.3 ± 0.9	10	5.8 ± 0.8	12	**0.0005**
TAPSE	0.35 ± 0.13	10	0.28 ± 0.11	12	0.1694
TR_{vel} (m s^{-1})	1.7 ± 0.4	9	2.7 ± 0.7	12	**0.0005**
LV ED eccentricity index	1.0 ± 0.1	10	1.2 ± 0.2	12	**0.0035**
LV ES eccentricity index	1.0 ± 0.1	10	1.3 ± 0.3	12	**0.0026**
Week 8					
Weight (kg)	17.3 ± 2.9	10	15.2 ± 1.9	10	0.0816
TAPSE	0.32 ± 0.06	9	0.32 ± 0.04	9	0.9311
TR_{vel} (m s^{-1})	1.7 ± 0.5	9	2.2 ± 0.6	9	0.0879
LV ED eccentricity index	1.0 ± 0.1	10	1.0 ± 0.1	9	0.5140
LV ES eccentricity index	1.0 ± 0.1	10	1.0 ± 0.1	9	0.9150
Week 5					
Weight (kg)	9.2 ± 1.0	9	7.3 ± 1.4	12	**0.0026**
Heart rate (bpm)	113 ± 35	9	107 ± 32	12	0.7059
Left ventricle					
End-diastolic volume (ml kg^{-1})	2.8 ± 0.6	9	3.6 ± 1.6	12	0.1480
End-systolic volume (ml kg^{-1})	1.4 ± 0.4	9	2.0 ± 1.2	12	0.1519
Ejection fraction (%)	52 ± 7	9	48 ± 10	12	0.3605
Mass (g kg^{-1})	2.1 ± 0.4	9	2.6 ± 0.6	12	**0.0222**
End-diastolic volume/mass (ml g^{-1})	1.3 ± 0.2	9	1.3 ± 0.3	12	0.9535
Stroke volume (ml $beat^{-1}$ kg^{-1})	1.4 ± 0.4	9	1.6 ± 0.5	12	0.2932
Cardiac index (l min^{-1} kg^{-1})	0.154 ± 0.029	9	0.166 ± 0.031	12	0.3956
Right ventricle					
End-diastolic volume (ml kg^{-1})	2.5 ± 0.6	9	3.1 ± 1.1	12	0.1242
End-systolic volume (ml kg^{-1})	1.0 ± 0.4	9	1.5 ± 0.7	12	0.0880
Ejection fraction (%)	59 ± 8	9	53 ± 9	12	0.1263
Mass (g kg^{-1})	0.73 ± 0.08	9	1.18 ± 0.36	12	**0.0019**
End-diastolic volume/mass (ml g^{-1})	3.4 ± 0.8	9	2.7 ± 0.4	12	**0.0138**
Global longitudinal strain (%)	26 ± 4	8	19 ± 5	12	**0.0044**
Week 12					
Weight (kg)	35 ± 5	6	27 ± 4	7	**0.0102**
Heart rate (bpm)	89 ± 7	6	89 ± 20	7	0.9169
Left ventricle					
End-diastolic volume (ml kg^{-1})	2.2 ± 0.4	6	2.4 ± 0.2	7	0.3224
End-systolic volume (ml kg^{-1})	0.8 ± 0.2	6	1.0 ± 0.1	7	0.1807
Ejection fraction (%)	63 ± 6	6	59 ± 7	7	0.1887
Mass (g kg^{-1})	1.92 ± 0.08	6	2.02 ± 0.21	7	0.4452
End-diastolic volume/mass (ml g^{-1})	1.2 ± 0.2	6	1.2 ± 0.2	7	0.6885
Stroke volume (ml $beat^{-1}$ kg^{-1})	1.4 ± 0.2	6	1.4 ± 0.3	7	0.9453
Cardiac index (l min^{-1} kg^{-1})	0.123 ± 0.017	6	0.122 ± 0.016	7	0.9013
Right ventricle					
End-diastolic volume (ml kg^{-1})	2.1 ± 0.3	6	2.1 ± 0.4	7	0.8678
End-systolic volume (ml kg^{-1})	0.7 ± 0.2	6	0.7 ± 0.1	7	0.8601
Ejection fraction (%)	65 ± 5	6	66 ± 4	7	0.7174
Mass (g kg^{-1})	0.81 ± 0.10	6	0.97 ± 0.11	7	**0.0183**
End-diastolic volume/mass (ml g^{-1})	2.6 ± 0.3	6	2.2 ± 0.2	7	**0.0232**
Global longitudinal strain (%)	25 ± 4	6	24 ± 3	7	0.4089

Values are mean ± SD. *P*-values shown in bold are statistically significant. Abbreviations: ED, end-diastolic; ES, end-systolic; LV, Left ventricle; NOI, neonatal oxidative injury; PAAT, pulmonary arterial acceleration time; TAPSE, tricuspid annular plane systolic excursion normalized to right ventricular length; TR_{vel}, tricuspid regurgitation peak velocity.

PVR during exercise at 4 km h^{-1} also correlated positively with duration of hypoxic exposure in 10- to 12-week-old piglets (Fig. 5). RV dP/dt_{max}, an index of contractility, was increased in NOI compared to SHAM piglets during exercise, likely due to the increased pulmonary artery pressure in NOI piglets (Table 3). Conversely, the rate of relaxation, RV dP/dt_{min} was unaltered in NOI piglets.

Alterations in nitric-oxide signalling

NOS inhibition with L-NNA resulted in an increase in PVR at rest, which was approximately twice as large in NOI compared to SHAM piglets (Fig. 6). In accordance with the larger increase in PVR in response to NOS inhibition, western blotting revealed increased total eNOS protein in bulk lung tissue of NOI, while p-eNOS/eNOS ratio was not different between SHAM and NOI (Fig. 7). No correlations were found with duration of hypoxic exposure or PVR. The PVR increased even further in NOI piglets during exercise, suggesting further impairment of vascular recruitment and vasodilator capacity during exercise following loss of NO.

PDE5i resulted in a significant decrease in PVR in both NOI and SHAM piglets. In contrast to control exercise, exercise in the presence of PDE5-i produced a further

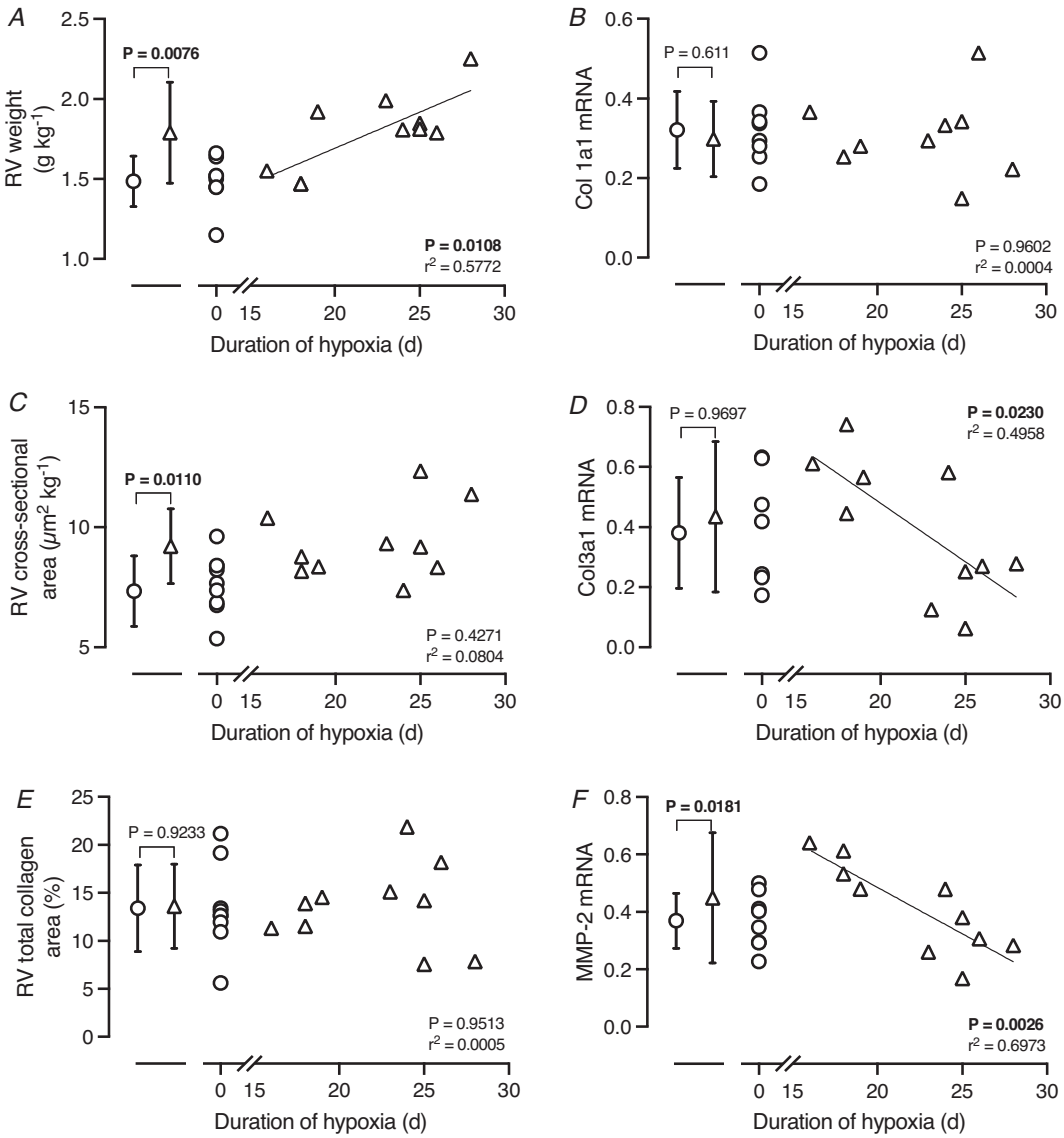

Figure 3. Influence of duration of postnatal hypoxia exposure on right ventricular (RV) tissue measurements
Only NOI animals are included in the regression analysis. mRNA expression was normalized using housekeeping genes cyclophilin A and β-actin. Data are shown as means ± SD and as individual data points as a function of duration of hypoxia; n = 8 for SHAM and n = 10 for NOI.

Table 3. Haemodynamics at rest and during exercise in 10–12 weeks old, chronically instrumented piglets subjected to neonatal oxidative injury (NOI) or SHAM procedure

At rest and during exercise		At rest	P^a	1 km h^{-1}	2 km h^{-1}	3 km h^{-1}	4 km h^{-1}	P^b
Heart rate (bpm)	SHAM	152 ± 13	0.7031	173 ± 15	188 ± 21	209 ± 19	245 ± 22	0.2336*
	NOI	155 ± 21		182 ± 31	200 ± 27	222 ± 26	252 ± 23	**<0.0001**†
								0.3040‡
Cardiac index (l min^{-1} kg^{-1})	SHAM	0.23 ± 0.04	0.3787	0.26 ± 0.04	0.29 ± 0.04	0.32 ± 0.04	0.35 ± 0.04	0.1460*
	NOI	0.22 ± 0.03		0.26 ± 0.04	0.28 ± 0.04	0.31 ± 0.04	0.35 ± 0.04	**<0.0001**†
								0.0730‡
Stroke volume (ml beat^{-1} kg^{-1})	SHAM	1.51 ± 0.25	0.6039	1.52 ± 0.22	1.53 ± 0.22	1.53 ± 0.23	1.44 ± 0.19	0.3298*
								0.1932†
	NOI	1.43 ± 0.29		1.46 ± 0.31	1.45 ± 0.31	1.45 ± 0.27	1.37 ± 0.22	0.5052‡
PAP (mmHg)	SHAM	14 ± 4	0.4833	19 ± 4	21 ± 4	23 ± 5	28 ± 5	**0.0010***
								<0.0001†
	NOI	16 ± 4		22 ± 6	24 ± 4	28 ± 4	33 ± 6	0.4471‡
LAP (mmHg)	SHAM	2 ± 3	0.1346	4 ± 3	6 ± 3	7 ± 2	9 ± 2	**<0.0001***
								<0.0001†
	NOI	0 ± 4		2 ± 3	2 ± 3	3 ± 4	4 ± 4	0.0683‡
PVR (mmHg min l^{-1} kg)	SHAM	54 ± 17	**0.0127**	54 ± 15	52 ± 14	51 ± 15	51 ± 16	**<0.0001***
								0.3605†
	NOI	73 ± 14		79 ± 19	80 ± 18	83 ± 20	83 ± 22	0.0746‡
MAP (mmHg)	SHAM	82 ± 7	0.6703	84 ± 7	84 ± 7	86 ± 8	88 ± 9	0.5938*
								0.0054†
	NOI	83 ± 5		86 ± 7	85 ± 5	88 ± 5	89 ± 4	0.3763‡
RV dPdt_{max} (mmHg s^{-1})	SHAM	1330 ± 257	0.1732	1646 ± 406	1758 ± 449	2076 ± 347	2606 ± 399	**0.0010***
								<0.0001†
	NOI	1563 ± 363		2005 ± 664	2214 ± 609	2484 ± 631	3121 ± 605	**0.9833**‡
RV dPdt_{min} (mmHg s^{-1})	SHAM	−863 ± 226	0.7615	−1165 ± 332	−1318 ± 379	−1664 ± 361	−2246 ± 371	0.8494*
								<0.0001†
	NOI	−834 ± 158		−1232 ± 234	−1421 ± 196	−1691 ± 214	−2290 ± 283	0.091‡
B$\dot{V}_{O_2}$ (ml min^{-1} kg^{-1})	SHAM	0.60 ± 0.10	0.3622	0.76 ± 0.09	0.91 ± 0.11	1.00 ± 0.14	1.31 ± 0.09	0.4884*
								<0.0001†
	NOI	0.55 ± 0.12		0.81 ± 0.09	0.90 ± 0.11	1.08 ± 0.09	1.33 ± 0.22	0.3550‡
Hypoxic challenge test		**Mean**[c]	P^a	**2 min**	**5 min**	**15 min**	**20 min**	P^b
Heart rate (bpm)	SHAM	158 ± 17	0.2466	184 ± 26	167 ± 25	139 ± 12	142 ± 16	0.9018*
								0.0035†
	NOI	174 ± 32		181 ± 26	177 ± 30	175 ± 46	159 ± 38	0.1662‡
Cardiac index (l min^{-1} kg^{-1})	SHAM	0.21 ± 0.05	0.9743	0.25 ± 0.06	0.23 ± 0.05	0.20 ± 0.05	0.20 ± 0.06	0.6230*
								0.0081†
	NOI	0.22 ± 0.03		0.23 ± 0.04	0.22 ± 0.03	0.21 ± 0.03	0.19 ± 0.05	0.7402‡

(*Continued*)

Table 3. (Continued)

Hypoxic challenge test		Mean[c]	P^a	2 min	5 min	15 min	20 min	P^b
Stroke volume (ml beat^{-1} kg^{-1})	SHAM	1.39 ± 0.41	0.5721	1.43 ± 0.55	1.37 ± 0.40	1.42 ± 0.34	1.39 ± 0.40	0.1247*
								0.6199†
	NOI	1.28 ± 0.30		1.30 ± 0.31	1.29 ± 0.27	1.29 ± 0.31	1.23 ± 0.30	0.7274‡
PAP (mmHg)	SHAM	24 ± 3	**0.0024**	26 ± 2	25 ± 5	22 ± 4	21 ± 5	**<0.0001***
								<0.0001†
	NOI	31 ± 4		37 ± 5	34 ± 6	31 ± 9	24 ± 6	**0.0419‡**
LAP (mmHg)	SHAM	5 ± 5	0.2466	4 ± 7	5 ± 5	5 ± 4	6 ± 6	**0.0353***
								0.7207†
	NOI	2 ± 5		1 ± 5	1 ± 6	2 ± 7	2 ± 4	0.9449‡
PVR (mmHg min l^{-1} kg)	SHAM	87 ± 26	**0.0016**	90 ± 44	94 ± 44	86 ± 21	75 ± 15	**<0.0001***
								0.0058†
	NOI	137 ± 21		158 ± 29	149 ± 24	130 ± 25	120 ± 22	0.5881‡
MAP (mmHg)	SHAM	89 ± 5	0.5023	88 ± 8	90 ± 5	90 ± 6	88 ± 7	0.5451*
								0.6061†
	NOI	93 ± 11		95 ± 11	92 ± 12	95 ± 11	92 ± 9	0.9529‡
RV dPdt_{max} (mmHg s^{-1})	SHAM	1667 ± 352	0.0983	2251 ± 617	1788 ± 412	1254 ± 1254	1415 ± 451	**<0.0001***
								0.0150†
	NOI	2061 ± 353		2406 ± 451	2120 ± 331	2054 ± 690	1781 ± 366	0.8848‡
RV dPdt_{min} (mmHg s^{-1})	SHAM	−943 ± 254	**0.0242**	−1043 ± 240	−1002 ± 245	−839 ± 247	−867 ± 321	**<0.0001***
								0.0150†
	NOI	−1271 ± 164		−1428 ± 196	−1326 ± 145	−1313 ± 316	−1083 ± 260	0.5305‡
Arterial oxygen tension (mmHg)	SHAM	57 ± 3	0.2469	44 ± 3	54 ± 4	63 ± 6	56 ± 8	0.9380*
								<0.0001†
	NOI	54 ± 5		47 ± 6	54 ± 6	57 ± 12	59 ± 12	0.8583‡
Arterial oxygen saturation (%)	SHAM	87 ± 3	0.4371	77 ± 3	87 ± 4	92 ± 4	87 ± 7	0.5001*
								0.0001†
	NOI	85 ± 3		78 ± 7	85 ± 5	87 ± 8	89 ± 8	0.5318‡

Values are mean ± SD, $n = 6$–7 for SHAM and $n = 10$ for NOI.
[a] t-test between groups.
[b] Mixed model repeated measures ANOVA with group as factor and $B\dot{V}_{O_2}$ (or heart rate in case of RV dPd$t_{max/min}$ or km h^{-1} in case of $B\dot{V}_{O_2}$) as covariate during exercise, and with time as covariate during hypoxic challenge test.
[c] Mean value of measurements at 2, 5, 10, 15 and 20 min of exposure to 14−15% fraction of inspired oxygen. P-values shown in bold indicate statistical significance.
* Difference between groups.
† Difference over time (during hypoxic challenge test) or km h^{-1} (during exercise).
‡ Interaction group × time or km h^{-1}. Abbreviations: $B\dot{V}_{O_2}$, body oxygen consumption; CI, cardiac index; dP/dt_{max}, maximum rate of rise of RV pressure; dP/dt_{min}, maximum rate of fall of RV pressure; LAP, left atrial pressure; MAP, mean arterial pressure; PAP, pulmonary arterial pressure; PVR, pulmonary vascular resistance; RV, right ventricle.

reduction in PVR in NOI piglets (Fig. 8). However, the reduction in PVR with PDE5-i was not accompanied by significant alterations in stroke volume in either group.

Discussion

The current study investigated the long-term effect of NOI on cardiopulmonary structure and function in piglets. The main findings were as follows. (1) CMR shortly after NOI showed increased RV mass and reduced GLS in NOI piglets compared to SHAM piglets. (2) After a normoxic recovery period of 6−8 weeks, resting PAP values of NOI piglets returned to SHAM values. Nevertheless, PVR remained elevated and RV hypertrophy persisted. (3) Both exercise and HCT unmasked left atrial under-filling and increased PAP as a consequence of an increase in PVR, in NOI piglets compared to SHAM. (4) During exercise, duration of neonatal hypoxic exposure correlated negatively with stroke volume whereas longer neonatal exposure to hypoxia attenuated or even negated the decrease in stroke volume during HCT. (5) NOI piglets demonstrated exaggerated PVR responses to either NOS or PDE5 inhibition compared to SHAM, implying a – possibly compensatory – increase in NO-cGMP signalling in NOI piglets.

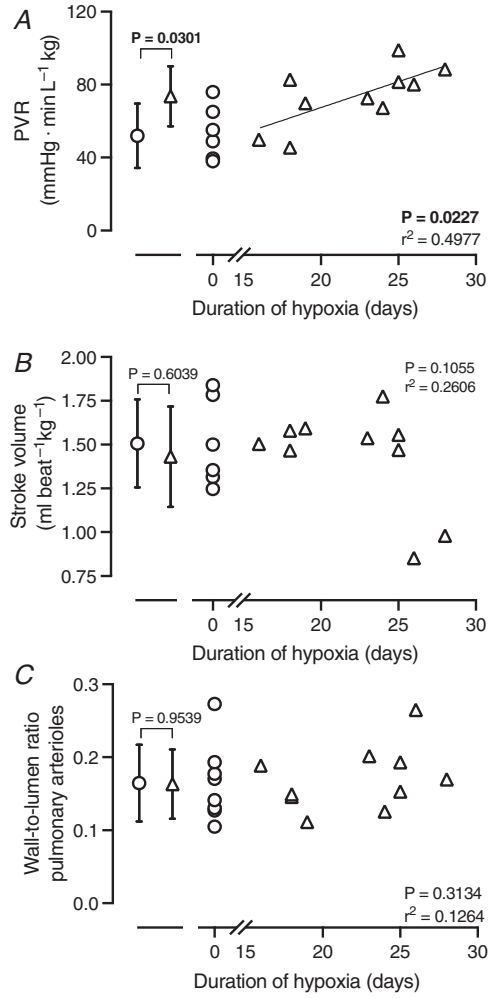

Figure 4. Influence of duration of hypoxia on pulmonary vascular resistance (PVR), stroke volume and wall-to-lumen ratio of pulmonary arterioles
Only NOI animals are included in the regression analysis. Data are shown as means ± SD and as individual data points plotted as a function of duration of hypoxia; n = 6–8 for SHAM and n = 10–11 for NOI.

Pulmonary vascular disease

It has been proposed that perinatal hits, such as hypoxic and hyperoxic episodes in preterm infants, predispose to development of PVD during life (de Wijs-Meijler et al., 2017). Secondary hits could induce further worsening of PVD and may even result in PAH with its devastating course of disease progression (Goss et al., 2017; Hoeper et al., 2017; McLaughlin & Suissa, 2010). Accordingly, Naumburg et al., showed an increased incidence of PAH in preterm born adults and children, while Goss et al., detected an early subclinical increase in PAP and PVR in preterm born young adults (Goss et al., 2018; Naumburg & Soderstrom, 2019). More than 20 years ago, Sartori et al. (1999) already showed exaggerated increases in PAP at high altitudes in adults with a history of perinatal pulmonary hypertension. More recently, Barton et al. (2021) observed an increased cardiac contractile response to hypoxia as measured by CMR, possibly induced by an exaggerated increase in afterload. Similarly, in our model, long-term PVD was unmasked by HCT and by exercise testing, as evidenced by an exaggerated increase in PVR and PAP. The increase in PVR during exercise was further exacerbated in the presence of NOS inhibition, whereas PDE5 inhibition produced a larger decrease in PVR in NOI *vs*. SHAM piglets. Together with the increased eNOS protein expression in the lungs, our data point towards an increased dependency on nitric oxide to blunt the effects of PVD on the pulmonary vasculature. Our observations are in accordance with data from Chao et al. (2018) that showed long-lasting histone modifications associated with an increased expression of *NOS3*, encoding eNOS protein, in a mouse model of neonatal hyperoxia. This suggests that there are compensatory mechanisms at play to reduce PAP at rest, using vasodilator capacity of the pulmonary vasculature, thereby exhausting reserve capacity during (physiological) stress. Importantly, nitric oxide signalling is dependent on a healthy pulmonary vascular endothelium, which is sensitive to common co-morbidities such as chronic kidney disease, obesity, smoking, ageing and LV heart disease (Goss et al., 2017). Nitric oxide dependency to maintain a low PVR, followed by a decrease in endothelial function due to unhealthy life style and/or

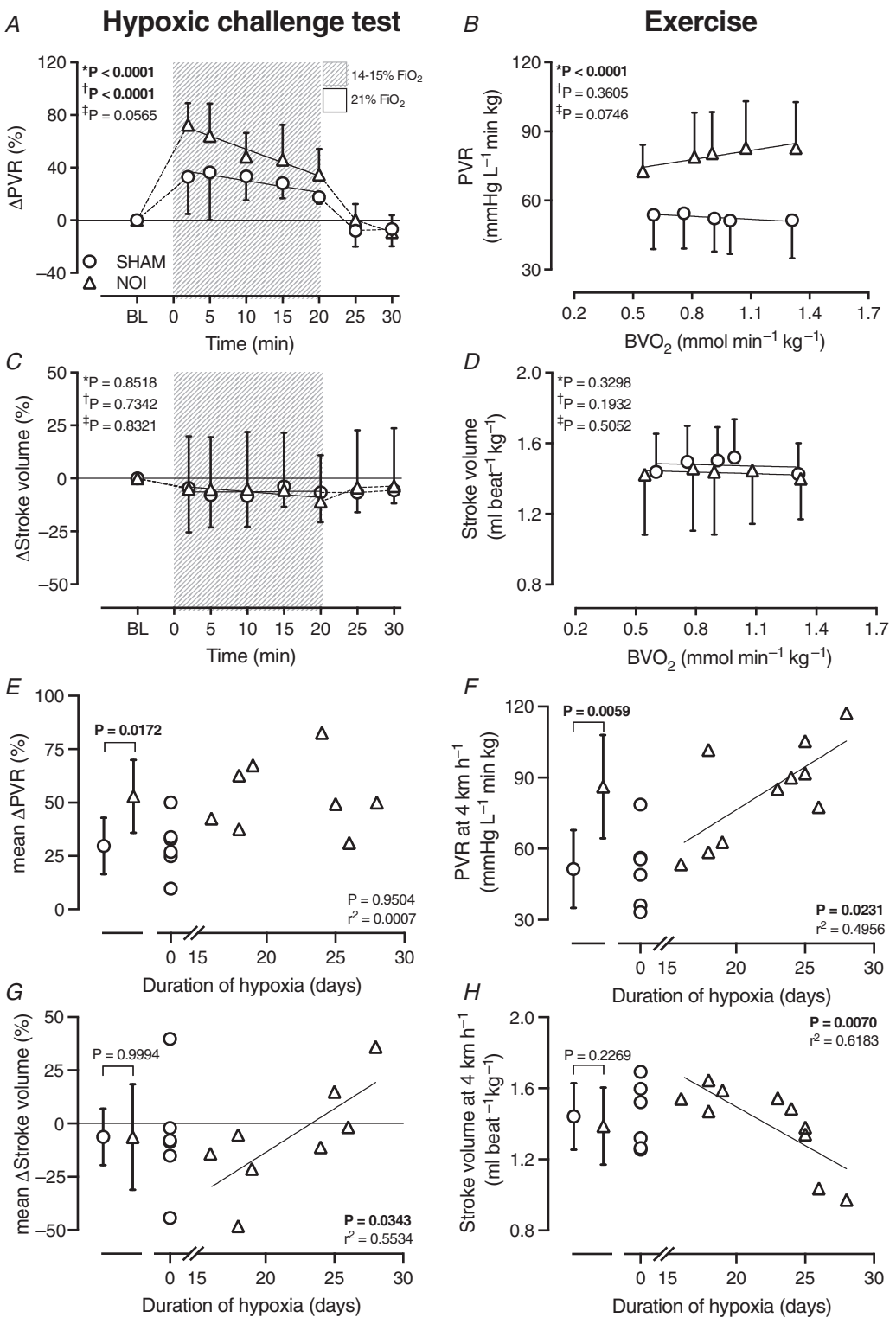

Figure 5. Pulmonary vascular resistance (PVR) and stroke volume during hypoxic challenge testing and exercise in 10- to 12-week-old, chronically instrumented piglets
Only NOI animals are included in the regression analysis. Data are shown as means ± SD and as individual data points plotted as a function of duration of hypoxia; n = 6–7 for SHAM and n = 8 for NOI. Mean Δ: Average change during hypoxic challenge test from measurements at 2, 5, 10, 15 and 20 min compared to baseline value. $B\dot{V}_{O_2}$, body oxygen consumption. *Difference between groups. †Difference over time or $B\dot{V}_{O_2}$. ‡Interaction group × time/$B\dot{V}_{O_2}$.

comorbid conditions, could be an important contributor to the progression of PVD in (young) adults with neonatal oxidative injury of the lungs. Future research should focus on pulmonary vascular function during stress and the role of second hits to the endothelium in preterm born young adults, to prevent the development of overt PAH later in life.

Right ventricular function and remodelling

Abnormalities in both LV and RV geometry and function have been observed in young adults born prematurely (Lewandowski, Augustine et al., 2013; Lewandowski, Bradlow et al., 2013). In general, RV function seems to be mostly affected in this population. However, given their connection via the pulmonary vasculature, as well as direct ventricular interactions, it is sometimes difficult to distinguish between RV and LV dysfunction. Altogether, our data suggest that NOI piglets develop RV hypertrophy in order to cope with the increased afterload of the RV during neonatal hypoxic exposure. This hypertrophy seems to be sufficient to maintain stroke volume at rest. Also, during re-exposure to hypoxia, the RV hypertrophy appears to be beneficial, as stroke volume was least affected in the NOI piglets with the longest exposure to neonatal hypoxia. Conversely, during exercise, stroke volume is lowest in these animals, which appears to be due to LV under-filling, evidenced by the lower LAP, during exercise. The reduction in atrioventricular pressure gradient can impair LV filling during exercise (Ruijsink et al., 2020; Schnell et al., 2017). Left atrial under-filling is a known feature of pulmonary hypertension, attributed to impaired RV function (Lumens et al., 2010; Sjogren et al., 2021). Similarly, several studies reported a decrease in LV diastolic function in preterm born young adults (Lewandowski et al., 2021). It is important to realize that LV relaxation correlates negatively with age, further impairing LV filling (Bryg et al., 1987). Future research should focus on the effect of risk profiles of preterm born young adults, and on the relative roles of NOI of the lung, RV dysfunction and impaired LV relaxation, in the reduced stroke volume.

The role of the duration of NOI on the cardiac phenotype later in life is currently not well-established, but is thought to be an important factor (Lewandowski, 2021). As mentioned above, in our study, extended exposure to oxidative injury in the neonatal phase increased RV mass, reduced stroke volume and cardiac index during exercise, but maintained stroke volume during HCT. Tissue analysis showed that prolonged hypoxic exposure was accompanied by a reduction in mRNA expression of the more compliant collagen type 3, but not in the dominant collagen type 1, which may have increased RV stiffness, independent of a change in total interstitial collagen area. Altogether, the functional, histological and molecular data suggest a remodelled, stiffer RV after prolonged exposure to hypoxia. This remodelled ventricle may be better equipped to deal with a 'static' increase in afterload (without extreme heart rate increase), such as during acute hypoxia, but less well equipped in dealing with

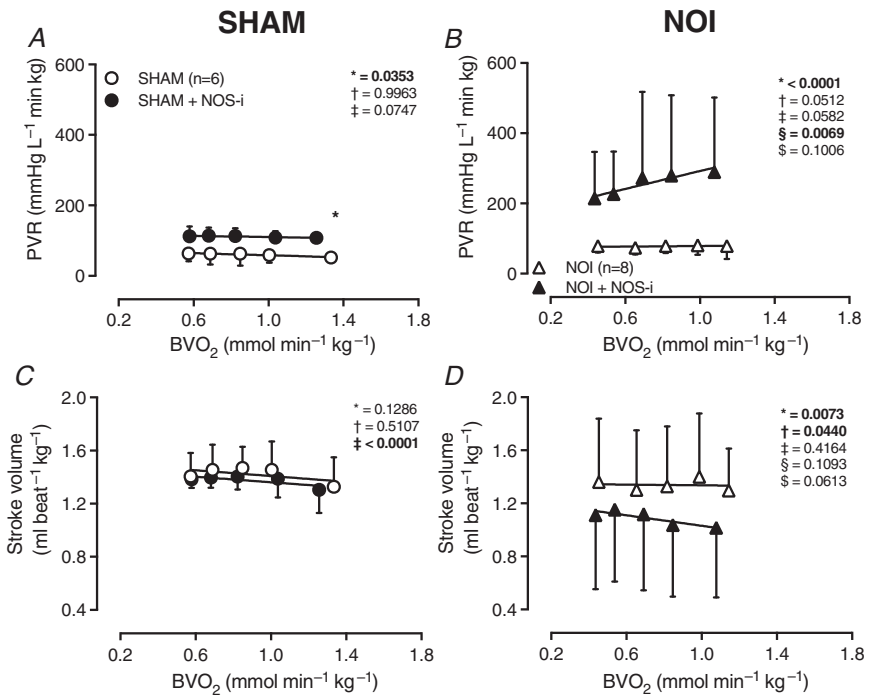

Figure 6. Inhibition of nitric oxide synthase (NOS-i) during exercise in 10- to 12-week-old, chronically instrumented piglets
NOI, neonatal oxidative injury piglets; PVR, pulmonary vascular resistance. Means ± SD are shown, n = 6 for SHAM and n = 8 for NOI at rest; in both groups one animal did not exercise. *NOS-i within group. †$B\dot{V}O_2$ within group. ‡Interaction NOS-i × $B\dot{V}O_2$ within groups. §NOS-i between groups. §Interaction NOS-i × $B\dot{V}O_2$ between groups.

'dynamic' increases in afterload such as during exercise (with heart rate increase). Our data are consistent with a rat model using neonatal hyperoxia to induce NOI. Rats with prolonged NOI (10 days) had a higher cardiac output upon adult re-exposure to hypoxia, compared to rats with short NOI time (4 days) and SHAM rats. This counter-intuitive beneficial effect was attributed to increased RV hypertrophic remodelling (Goss et al., 2015). Similar phenotypes have been described in extremely preterm born young adults. Lewandowski *et al.* showed an increased RV mass, while Barton et al., reported an exaggerated RV response to hypoxia by CMR (Barton et al., 2021; Lewandowski, Bradlow et al., 2013). Such RV remodelling has been proposed to be beneficial for late events (Sanz et al., 2019). Yet, it may also mask early signs of PVD in this population, increase time to diagnosis and thereby worsen outcomes (Gaine et al., 2021; Vachiery & Gaine, 2012).

Clinical relevance

During the Sixth World Symposium on pulmonary hypertension, exercise pulmonary hypertension was not reintroduced in the diagnostic guidelines (Galie et al., 2019). The taskforce declared that accurate right heart catheterization measurements are challenging to obtain and are unable to differentiate between pulmonary arterial wedge pressure and PVD as a possible cause of exercise pulmonary hypertension. However, this large animal study shows that functional cardiovascular testing could be of additional value to phenotyping cardiovascular responses in adults with NOI of the pulmonary circulation. Combining exercise or hypoxia with (preferably non-invasive) cardiac volume or pressure measurements is logistically challenging, but has been performed in experimental and clinical settings and provides diagnostic and prognostic value (Backhaus et al., 2021; Barton et al., 2021; Craven et al., 2020; Huckstep et al., 2021; Le et al., 2020; Macdonald et al., 2021; Ruijsink et al., 2020). In a preterm born population, MacDonald et al., showed impaired RV filling using 4D flow CMR during exercise, while Huckstep et al., detected decreases in LV ejection fraction during exercise (Huckstep et al., 2018, 2021; Macdonald et al., 2021). Barton et al., combined hypoxia with CMR (Barton et al., 2021). Large scale cohorts should be subjected to these tests during young adulthood, in order to determine pathophysiological factors that could deteriorate to overt, adult PAH or heart failure.

Without clear end-points, designing treatments for adolescents/young adults exposed to NOI is challenging. In a recent pilot study by Corrado *et al.*, acute treatment with sildenafil improved cardiac index as measured with 4D flow CMR (Corrado, Barton, Francois et al., 2021). PDE5 inhibition using sildenafil is registered for treatment of adult PAH. For paediatric PVD, however, PDE5 treatment is controversial (Abman et al., 2013). Future studies should determine whether PDE5 inhibition could be used as a prophylactic or therapeutic approach in subsets of young adult survivors of NOI, particularly when at risk for PAH.

In 2019, the European Respiratory Society recommended exercise training in severe chronic pulmonary hypertension patients. Exercise was shown to be safe, cost-efficient and effective in improving exercise capacity, quality of life and (pulmonary) haemodynamics (Grunig et al., 2019). In young, preterm born children (aged 4–6 years), diagnosed with bronchopulmonary dysplasia, exercise training improved exercise capacity (Morales Mestre et al., 2018). However, it remains to be demonstrated whether exercise merely improves RV function, thereby potentially masking early PVD symptoms – which could lead to underdiagnosis and eventually to adverse outcomes – or that the pulmonary circulation itself also benefits from exercise training.

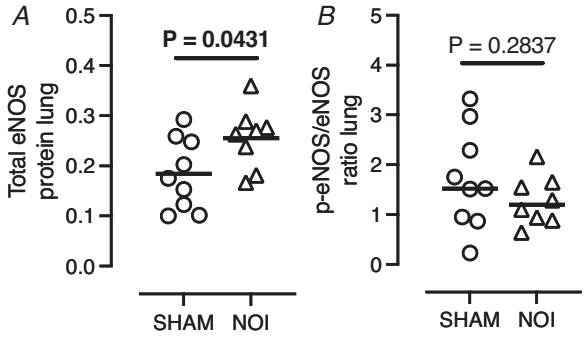

Figure 7. Total endothelial nitric oxide synthase (eNOS) protein normalized to GAPDH and phosphorylated eNOS (p-eNOS)/eNOS ratio in lung tissue in 10- to 12-week-old, chronically instrumented swine
NOI, neonatal oxidative injury piglets. Shown are individual data points ($n = 9$ for SHAM and $n = 8$ for NOI). Mean values are denoted by the horizontal lines. Original Western blots are shown in the supplementary data.

Strengths and limitations

This work presents a comprehensive study into the late cardiopulmonary response to NOI in swine, integrating pulmonary vascular and RV structure and function. It provides extensive cardiac imaging combined with invasive measurements combined with exposure to multiple stressors for the pulmonary circulation. It is important to note that duration of hypoxia exposure was dependent on clinical symptoms and was therefore influenced by the capacity of the RV to adapt to the increase in afterload induced by hypoxia. Consequently,

the correlations between duration of hypoxia with RV and pulmonary vascular responses to exercise and re-exposure to hypoxia later in life could be the result of prolonged exposure to the high PAP, but likely also reflect differences in pathways that may contribute to the vulnerability to develop PVD and RV dysfunction. Indeed, prolonged exposure to NOI was associated with a better cardiopulmonary response to renewed hypoxia exposure, but a worse response to exercise. Although unlikely, it is also possible that the duration of the recovery may have influenced the results. Shorter exposure to hypoxia led - by design - to a longer recovery period, and resulted in a phenotype that, at rest, resembled the control animals more in terms of PVR and SV, but not in RV weight, cardiomyocyte size, total collagen or expression of COL3a1 and MMP-2.

Clinically, cardiopulmonary development of premature born infants is compromised by multiple hits, both antenatally (i.e. intra uterine growth restriction and infection), and postnatally (NOI and postnatal infections). In this study, we focused on the influence of NOI on a young, developing cardiopulmonary system, thereby simplifying the complexity of the hits. Other studies have used (premature) sheep, thereby including infection, placental insufficiency, maternal undernutrition or chronic hypoxaemia as a factor, but with more limited follow-up duration (Botting et al., 2014; Darby et al., 2018, 2020, 2022; Vrselja et al., 2022). More complex models with multiple hits clearly have the advantage that they mimic the clinical situation more closely. However, in such complex models, the influence of each individual hit is more difficult to delineate.

This study investigated cardiopulmonary response to NOI in swine until 3 months of age, which in terms of weight is equivalent to a 10-year-old child. Kumari et al. subjected neonatal rats to 85% hyperoxia for 14 days. At day 90, rats seemed recovered, but deteriorated at day 365 (Kumari et al., 2019). In our model, the progression of PVD and/or RV dysfunction later in life are unknown and remain to be investigated.

Conclusions and future directions

The present study is the first to use a large animal model to investigate the influence of perinatal oxidative injury on pulmonary arterial and RV function and structure in 10- to 12-week-old piglets, at rest, during exercise and during HCT. Exercise and HCT unmasked left atrial under-filling, as well as increased PVR and nitric oxide dependency. Age- or comorbidity-related loss of pulmonary endothelial function in combination with an increased nitric oxide dependency in the pulmonary circulation after NOI could therefore be a pathophysiological mechanism in the development of adult PAH after NOI.

Duration of hypoxic exposure correlated negatively with stroke volume during exercise, but positively during HCT. These findings indicate that there are distinct functional and structural cardiopulmonary phenotypes after exposure to NOI. Hence, testing the functional cardiopulmonary adaptive response to various stressors could be useful in stratifying adolescents or young adults after NOI.

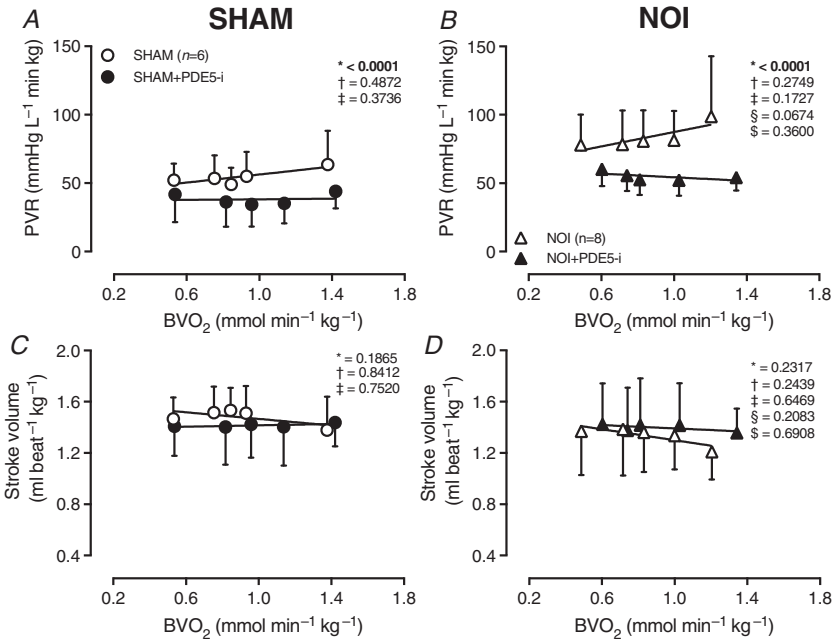

Figure 8. Inhibition of phosphodiesterase 5 (PDE5-i) at rest and during exercise in 10- to 12-week-old, chronically instrumented piglets
NOI, neonatal oxidative injury piglets; PVR, pulmonary vascular resistance. Mean ± SD are shown, n = 6 for SHAM and n = 8 for NOI. *PDE5-i within group. †$B\dot{V}_{O_2}$ within group. ‡Interaction PDE5-i × $B\dot{V}_{O_2}$ within groups. §PDE5-i between groups. §Interaction PDE5-i × $B\dot{V}_{O_2}$ between groups.

References

Abman, S. H., Kinsella, J. P., Rosenzweig, E. B., Krishnan, U., Kulik, T., Mullen, M., Wessel, D. L., Steinhorn, R., Adatia, I., Hanna, B., Feinstein, J., Fineman, J., Raj, U., & Humpl, T., & Pediatric Pulmonary Hypertension N (2013). Implications of the U.S. Food and Drug Administration warning against the use of sildenafil for the treatment of pediatric pulmonary hypertension. *American Journal of Respiratory and Critical Care Medicine*, **187**(6), 572–575.

Backhaus, S. J., Lange, T., George, E. F., Hellenkamp, K., Gertz, R. J., Billing, M., Wachter, R., Steinmetz, M., Kutty, S., Raaz, U., Lotz, J., Friede, T., Uecker, M., Hasenfuss, G., Seidler, T., & Schuster, A. (2021). Exercise-stress real-time cardiac magnetic resonance imaging for non-invasive characterisation of heart failure with preserved ejection fraction: The HFpEF stress trial. *Circulation*, **143**(15), 1484–1498.

Barton, G. P., Corrado, P. A., Francois, C. J., Chesler, N. C., Eldridge, M. W., Wieben, O., & Goss, K. N. (2021). Exaggerated cardiac contractile response to hypoxia in adults born preterm. *Journal of Clinical Medicine*, **10**(6), 1166.

Bates, M. L., Levy, P. T., Nuyt, A. M., Goss, K. N., Lewandowski, A. J., & McNamara, P. J. (2020). Adult Cardiovascular health risk and cardiovascular phenotypes of prematurity. *Journal of Pediatrics*, **227**, 17–30.

Botting, K. J., McMillen, I. C., Forbes, H., Nyengaard, J. R., & Morrison, J. L. (2014). Chronic hypoxemia in late gestation decreases cardiomyocyte number but does not change expression of hypoxia-responsive genes. *Journal of the American Heart Association*, **3**(4), e000531.

Bryg, R. J., Williams, G. A., & Labovitz, A. J. (1987). Effect of aging on left ventricular diastolic filling in normal subjects. *American Journal of Cardiology*, **59**(9), 971–974.

Bustin, S. A., Benes, V., Garson, J. A., Hellemans, J., Huggett, J., Kubista, M., Mueller, R., Nolan, T., Pfaffl, M. W., Shipley, G. L., Vandesompele, J., & Wittwer, C. T. (2009). The MIQE guidelines: Minimum information for publication of quantitative real-time PCR experiments. *Clinical Chemistry*, **55**(4), 611–622

Chao, C. M., van den Bruck, R., Lork, S., Merkle, J., Krampen, L., Weil, P. P., Aydin, M., Bellusci, S., Jenke, A. C., & Postberg, J. (2018). Neonatal exposure to hyperoxia leads to persistent disturbances in pulmonary histone signatures associated with NOS3 and STAT3 in a mouse model. *Clinical Epigenetics*, **10**(1), 37.

Corrado, P. A., Barton, G. P., Francois, C. J., Wieben, O., & Goss, K. N. (2021). Sildenafil administration improves right ventricular function on 4D flow MRI in young adults born premature. *American Journal of Physiology. Heart and Circulatory Physiology*, **320**(6), H2295–H2304.

Corrado, P. A., Barton, G. P., Macdonald, J. A., Francois, C. J., Eldridge, M. W., Goss, K. N., & Wieben, O. (2021). Altered right ventricular filling at four-dimensional flow MRI in young adults born prematurely. *Radiology: Cardiothoracic Imaging*, **3**, e200618.

Craven, T. P., Tsao, C. W., La Gerche, A., Simonetti, O. P., & Greenwood, J. P. (2020). Exercise cardiovascular magnetic resonance: Development, current utility and future applications. *Journal of Cardiovascular Magnetic Resonance*, **22**(1), 65.

Crispi, F., Rodriguez-Lopez, M., Bernardino, G., Sepulveda-Martinez, A., Prat-Gonzalez, S., Pajuelo, C., Perea, R. J., Caralt, M. T., Casu, G., Vellve, K., Crovetto, F., Burgos, F., De Craene, M., Butakoff, C., Gonzalez Ballester, M. A., Blanco, I., Sitges, M., Bijnens, B., & Gratacos, E. (2021). Exercise capacity in young adults born small for gestational age. *JAMA Cardiology*, **6**(11), 1308.

Crump, C., Howell, E. A., Stroustrup, A., McLaughlin, M. A., Sundquist, J., & Sundquist, K. (2019). Association of preterm birth with risk of ischemic heart disease in adulthood. *JAMA Pediatrics*, **173**(8), 736–743.

Darby, J. R. T., Chiu, J., Regnault, T. R. H., & Morrison, J. L. (2022). Placental insufficiency induces a sexually dimorphic response in the expression of cardiac growth and metabolic signalling molecules upon exposure to a postnatal western diet in guinea pigs. *Journal of Developmental Origins of Health and Disease*, **13**(3), 345–357.

Darby, J. R. T., McMillen, I. C., & Morrison, J. L. (2018). Maternal undernutrition in late gestation increases IGF2 signalling molecules and collagen deposition in the right ventricle of the fetal sheep heart. *Journal of Physiology*, **596**(12), 2345–2358.

Darby, J. R. T., Varcoe, T. J., Orgeig, S., & Morrison, J. L. (2020). Cardiorespiratory consequences of intrauterine growth restriction: Influence of timing, severity and duration of hypoxaemia. *Theriogenology*, **150**, 84–95.

de Wijs-Meijler, D. P., Duncker, D. J., Tibboel, D., Schermuly, R. T., Weissmann, N., Merkus, D., & Reiss, I. K. M. (2017). Oxidative injury of the pulmonary circulation in the perinatal period: Short- and long-term consequences for the human cardiopulmonary system. *Pulmonary Circulation*, **7**(1), 55–66.

De Wijs-Meijler, D. P., Stam, K., van Duin, R. W., Verzijl, A., Reiss, I. K., Duncker, D. J., & Merkus, D. (2016). Surgical placement of catheters for long-term cardiovascular exercise testing in swine. *Journal of Visualized Experiments*, e53772.

de Wijs-Meijler, D. P. M., van Duin, R. W. B., Duncker, D. J., Scherrer, U., Sartori, C., Reiss, I. K. M., & Merkus, D. (2018). Structural and functional changes of the pulmonary vasculature after hypoxia exposure in the neonatal period: A new swine model of pulmonary vascular disease. *American Journal of Physiology. Heart and Circulatory Physiology*, **314**, H603–H615.

Duke, J. W., Lewandowski, A. J., Abman, S. H., & Lovering, A. T. (2021). Physiological aspects of cardiopulmonary dysanapsis on exercise in adults born preterm. *Journal of Physiology*, **600**(3), 463–482.

Gaine, S., Sitbon, O., Channick, R. N., Chin, K. M., Sauter, R., Galie, N., Hoeper, M. M., McLaughlin, V. V., Preiss, R., Rubin, L. J., Simonneau, G., Tapson, V., Ghofrani, H. A., & Lang, I. (2021). Relationship between time from diagnosis and morbidity/mortality in pulmonary arterial hypertension: Results from the phase III GRIPHON study. *Chest*, **160**(1), 277–286.

Galie, N., McLaughlin, V. V., Rubin, L. J., & Simonneau, G. (2019). An overview of the 6th world symposium on pulmonary hypertension. *European Respiratory Journal*, **53**(1), 1802148.

Goss, K. N., Beshish, A. G., Barton, G. P., Haraldsdottir, K., Levin, T. S., Tetri, L. H., Battiola, T. J., Mulchrone, A. M., Pegelow, D. F., Palta, M., Lamers, L. J., Watson, A. M., Chesler, N. C., & Eldridge, M. W. (2018). Early pulmonary vascular disease in young adults born preterm. *American Journal of Respiratory and Critical Care Medicine*, **198**(12), 1549–1558.

Goss, K. N., Cucci, A. R., Fisher, A. J., Albrecht, M., Frump, A., Tursunova, R., Gao, Y., Brown, M. B., Petrache, I., Tepper, R. S., Ahlfeld, S. K., & Lahm, T. (2015). Neonatal hyperoxic lung injury favorably alters adult right ventricular remodeling response to chronic hypoxia exposure. *American Journal of Physiology. Lung Cellular and Molecular Physiology*, **308**(8), L797–L806.

Goss, K. N., & Eldridge, M. W. (2021). Exploring the cardiac phenotypes of prematurity-reply. *JAMA Cardiology*, **6**(3), 361–362.

Goss, K. N., Everett, A. D., Mourani, P. M., Baker, C. D., & Abman, S. H. (2017). Addressing the challenges of phenotyping pediatric pulmonary vascular disease. *Pulmonary Circulation*, **7**(1), 7–19.

Goss, K. N., Haraldsdottir, K., Beshish, A. G., Barton, G. P., Watson, A. M., Palta, M., Chesler, N. C., Francois, C. J., Wieben, O., & Eldridge, M. W. (2020). Association between preterm birth and arrested cardiac growth in adolescents and young adults. *JAMA Cardiology*, **5**(8), 910–919.

Greer, C., Troughton, R. W., Adamson, P. D., & Harris, S. L. (2021). Preterm birth and cardiac function in adulthood. *Heart*, **108**(3), 172–177.

Grunig, E., Eichstaedt, C., Barbera, J. A., Benjamin, N., Blanco, I., Bossone, E., Cittadini, A., Coghlan, G., Corris, P., D'Alto, M., D'Andrea, A., Delcroix, M., de Man, F., Gaine, S., Ghio, S., Gibbs, S., Gumbiene, L., Howard, L. S., Johnson, M., … Peacock, A. J. (2019). ERS statement on exercise training and rehabilitation in patients with severe chronic pulmonary hypertension. *European Respiratory Journal*, **53**(2), 1800332.

Hoeper, M. M., Kramer, T., Pan, Z., Eichstaedt, C. A., Spiesshoefer, J., Benjamin, N., Olsson, K. M., Meyer, K., Vizza, C. D., Vonk-Noordegraaf, A., Distler, O., Opitz, C., Gibbs, J. S. R., Delcroix, M., Ghofrani, H. A., Huscher, D., Pittrow, D., Rosenkranz, S., & Grunig, E. (2017). Mortality in pulmonary arterial hypertension: Prediction by the 2015 European pulmonary hypertension guidelines risk stratification model. *European Respiratory Journal*, **50**(2), 1700740.

Huckstep, O. J., Burchert, H., Williamson, W., Telles, F., Tan, C. M. J., Bertagnolli, M., Arnold, L., Mohamed, A., McCormick, K., Hanssen, H., Leeson, P., & Lewandowski, A. J. (2021). Impaired myocardial reserve underlies reduced exercise capacity and heart rate recovery in preterm-born young adults. *European Heart Journal Cardiovascular Imaging*, **22**(5), 572–580.

Huckstep, O. J., Williamson, W., Telles, F., Burchert, H., Bertagnolli, M., Herdman, C., Arnold, L., Smillie, R., Mohamed, A., Boardman, H., McCormick, K., Neubauer, S., Leeson, P., & Lewandowski, A. J. (2018). Physiological stress elicits impaired left ventricular function in preterm-born adults. *Journal of the American College of Cardiology*, **71**(12), 1347–1356.

Kumari, S., Braun, R. K., Tetri, L. H., Barton, G. P., Hacker, T. A., & Goss, K. N. (2019). Bimodal right ventricular dysfunction after postnatal hyperoxia exposure: Implications for the preterm heart. *American Journal of Physiology. Heart and Circulatory Physiology*, **317**(6), H1272–H1281.

Le, T. T., Bryant, J. A., Ang, B. W. Y., Pua, C. J., Su, B., Ho, P. Y., Lim, S., Huang, W., Lee, P. T., Tang, H. C., Chin, C. T., Tan, B. Y., Cook, S. A., & Chin, C. W. (2020). The application of exercise stress cardiovascular magnetic resonance in patients with suspected dilated cardiomyopathy. *Journal of Cardiovascular Magnetic Resonance*, **22**(1), 10.

Lewandowski, A. J. (2021). The preterm (Right) heart: Does bronchopulmonary dysplasia play a unique role in long-term remodeling? *Chest*, **160**(1), 27–28.

Lewandowski, A. J., Augustine, D., Lamata, P., Davis, E. F., Lazdam, M., Francis, J., McCormick, K., Wilkinson, A. R., Singhal, A., Lucas, A., Smith, N. P., Neubauer, S., & Leeson, P. (2013). Preterm heart in adult life: Cardiovascular magnetic resonance reveals distinct differences in left ventricular mass, geometry, and function. *Circulation*, **127**(2), 197–206.

Lewandowski, A. J., Bradlow, W. M., Augustine, D., Davis, E. F., Francis, J., Singhal, A., Lucas, A., Neubauer, S., McCormick, K., & Leeson, P. (2013). Right ventricular systolic dysfunction in young adults born preterm. *Circulation*, **128**(7), 713–720.

Lewandowski, A. J., & Levy, P. T. (2021). Exploring the cardiac phenotypes of prematurity. *JAMA Cardiology*, **6**(3), 361.

Lewandowski, A. J., Raman, B., Bertagnolli, M., Mohamed, A., Williamson, W., Pelado, J. L., McCance, A., Lapidaire, W., Neubauer, S., & Leeson, P. (2021). Association of preterm birth with myocardial fibrosis and diastolic dysfunction in young adulthood. *Journal of the American College of Cardiology*, **78**(7), 683–692.

Lumens, J., Blanchard, D. G., Arts, T., Mahmud, E., & Delhaas, T. (2010). Left ventricular underfilling and not septal bulging dominates abnormal left ventricular filling hemodynamics in chronic thromboembolic pulmonary hypertension. *American Journal of Physiology. Heart and Circulatory Physiology*, **299**(4), H1083–H1091.

Macdonald, J. A., Roberts, G. S., Corrado, P. A., Beshish, A. G., Haraldsdottir, K., Barton, G. P., Goss, K. N., Eldridge, M. W., Francois, C. J., & Wieben, O. (2021). Exercise-induced irregular right heart flow dynamics in adolescents and young adults born preterm. *Journal of Cardiovascular Magnetic Resonance*, **23**(1), 116.

McKay, L., Goss, K. N., Haraldsdottir, K., Beshish, A. G., Barton, G. P., Palta, M., Chesler, N. C., Francois, C. J., Wieben, O., Macdonald, J. A., Eldridge, M. W., & Watson, A. M. (2021). Decreased ventricular size and mass mediate the reduced exercise capacity in adolescents and adults born premature. *Early Human Development*, **160**, 105426.

McLaughlin, V. V., & Suissa, S. (2010). Prognosis of pulmonary arterial hypertension: The power of clinical registries of rare diseases. *Circulation*, **122**(2), 106–108.

Morales Mestre, N., Papaleo, A., Morales Hidalgo, V., Caty, G., & Reychler, G. (2018). Physical activity program improves functional exercise capacity and flexibility in extremely preterm children with bronchopulmonary dysplasia aged 4–6 years: A randomized controlled trial. *Archivos de Bronconeumologia (English Edition)*, **54**, 607–613.

Naumburg, E., & Soderstrom, L. (2019). Increased risk of pulmonary hypertension following premature birth. *BMC Pediatrics*, **19**, 288.

Ruijsink, B., Forte, M. N. V., Duong, P., Asner, L., Pushparajah, K., Frigiola, A., Nordsletten, D., & Razavi, R. (2020). Synergy in the heart: RV systolic function plays a key role in optimizing LV performance during exercise. *American Journal of Physiology. Heart and Circulatory Physiology*, **319**(3), H642–H650.

Sanz, J., Sanchez-Quintana, D., Bossone, E., Bogaard, H. J., & Naeije, R. (2019). Anatomy, function, and dysfunction of the right ventricle: JACC state-of-the-art review. *Journal of the American College of Cardiology*, **73**(12), 1463–1482.

Sartori, C., Allemann, Y., Trueb, L., Delabays, A., Nicod, P., & Scherrer, U. (1999). Augmented vasoreactivity in adult life associated with perinatal vascular insult. *Lancet*, **353**(9171), 2205–2207.

Schnell, F., Claessen, G., La Gerche, A., Claus, P., Bogaert, J., Delcroix, M., Carre, F., & Heidbuchel, H. (2017). Atrial volume and function during exercise in health and disease. *Journal of Cardiovascular Magnetic Resonance*, **19**(1), 104.

Sjogren, H., Kjellstrom, B., Bredfelt, A., Steding-Ehrenborg, K., Radegran, G., Hesselstrand, R., Arheden, H., & Ostenfeld, E. (2021). Underfilling decreases left ventricular function in pulmonary arterial hypertension. *International Journal of Cardiovascular Imaging*, **37**(5), 1745–1755.

Telles, F., McNamara, N., Nanayakkara, S., Doyle, M. P., Williams, M., Yaeger, L., Marwick, T. H., Leeson, P., Levy, P. T., & Lewandowski, A. J. (2020). Changes in the preterm heart from birth to young adulthood: A meta-analysis. *Pediatrics*, **146**(2), e20200146.

Vachiery, J. L., & Gaine, S. (2012). Challenges in the diagnosis and treatment of pulmonary arterial hypertension. *European Respiratory Review*, **21**(126), 313–320.

van de Wouw, J., Steenhorst, J. J., Sorop, O., van Drie, R. W. A., Wielopolski, P. A., Kleinjan, A., Hirsch, A., Duncker, D. J., & Merkus, D. (2021). Impaired pulmonary vasomotor control in exercising swine with multiple comorbidities. *Basic Research in Cardiology*, **116**(1), 51.

Vrselja, A., Pillow, J. J., Bensley, J. G., Ellery, S. J., Ahmadi-Noorbakhsh, S., Moss, T. J., & Black, M. J. (2022). Intrauterine inflammation exacerbates maladaptive remodeling of the immature myocardium after preterm birth in lambs. *Pediatric Research*.

Zoller, B., Sundquist, J., Sundquist, K., & Crump, C. (2015). Perinatal risk factors for premature ischaemic heart disease in a Swedish national cohort. *BMJ Open*, **5**, e007308.

Additional information

Data availability statement

All data are available as supporting online information to the paper.

Competing interests

None.

Author contributions

J.S., A.H., D.d.W., D.D., I.R. and D.W. conceptualized the experiments, J.S., A.H., A.V. and P.W. performed the experiments, and J.S. and D.M. drafted the initial manuscript. All authors have read, revised and approved the final version of this manuscript and agree to be accountable for all aspects of the work in ensuring that questions related to the accuracy or integrity of any part of the work are appropriately investigated and resolved. All persons designated as authors qualify for authorship, and all those who qualify for authorship are listed.

Funding

This work was funded by DZHK; 81Z0600207 to D.M., The Sophia foundation S13-12 to D.d.W., Erasmus MC grant – 2016-15 to D.M.

Acknowledgements

The authors thank Esther van de Kamp, Lau Blonden, Ilona Krabbendam, Metin Sahin, Geraldine de Bruine, Matthijs Kuijpers, Marjolein Mol, Francis Pauletta, Remon Jansen, Bram van Liemde, Joey Gooshouwer and Chayenne Heijerman for their expert technical support.

Keywords

heart failure, neonatal, pulmonary vascular disease

Supporting information

Additional supporting information can be found online in the Supporting Information section at the end of the HTML view of the article. Supporting information files available:

Statistical Summary Document
Peer Review History
Original Western blots